High Temperature Sorption Separation of Air for Producing Oxygen-Enriched CO_2 Stream

Qing Yang and Y. S. Lin
Dept. of Chemical and Materials Engineering, University of Cincinnati, Cincinnati, OH 45221 and
Dept. of Chemical and Materials Engineering, Arizona State University, Tempe, AZ 85287

Martin Bülow
The BOC Group, PGS Technology, 100 Mountain Avenue, Murray Hill, NJ 07974

DOI 10.1002/aic.10638
Published online October 13, 2005 in Wiley InterScience (www.interscience.wiley.com).

A new high temperature sorption process for production of oxygen-enriched carbon dioxide stream through air separation with carbon dioxide as the purge gas is reported. The process is based on a fixed-bed packed with a perovskite-type strontium-iron doped lanthanum cobaltite, as the sorbent, operated in 500–900°C. Oxygen is adsorbed by the perovskite-type sorbent with air being fed. An oxygen-enriched carbon dioxide stream is obtained when the fixed-bed is regenerated with carbon dioxide as the desorption gas. A specific carbonation-reaction mechanism for the O_2-desorption process and a complete reverse reaction during the O_2-sorption process are identified with the evidences of XRD and TGA analysis. A study of the sorption process kinetics over a temperature range of 600–800°C was conducted by fixed-bed sorption/desorption and TGA experiments. Both desorption and sorption processes exhibit a high reaction rate in an initial stage followed by a slower rate in a second stage. A remarkable separation efficiency was observed at 800°C. The new process offers potential for applications in a number of processes including in the efficient and environmentally benign oxyfuel coal combustion process for power generation. © 2005 American Institute of Chemical Engineers *AIChE J,* 52: 574–581, 2006

Keywords: perovskite-type ceramic, type; carbon dioxide; air separation; sorption; desorption; carbonation; sorption kinetics

Introduction

Several perovskite-type oxides offer potential as sorbents for O_2 production *via* high-temperature air separation.[1,2] The new sorption separation process takes advantage of unique properties of certain perovskite-type ceramics that can adsorb a large quantity of O_2, but no other gases, at high temperatures. The sorption and desorption mechanism is based on the following reversible defect reaction[3,4,5]

$$1/2\ O_2(g) + V_o^{\cdot\cdot} \Leftrightarrow O_o^{\times} + 2h^{\cdot} \qquad \text{(A)}$$

in which $V_o^{\cdot\cdot}$, $O_o^{\times}$ and $h^{\cdot}$ denote positive oxygen vacancy, neutralized lattice oxygen, and mobile electronic hole, respectively. Main features of this new type of sorbents include infinitely large oxygen selectivity, relatively high-sorption capacity and high-sorption rate. Novel O_2-sorption processes could be developed utilizing these sorbents. Related processes may find widespread applications in air separation,[6] trace-O_2 removal, and other applications that involve high-temperature operations, including those of the membrane-separation principle.[5,7]

The new O_2-sorption process for gas separations was first

Correspondence concerning this article should be addressed to J. Y. S. Lin at Jerry.lin@asu.edu

proposed by Lin et al.[8] Fundamental studies on perovskite-type oxides comprise selection and syntheses of materials, determination of their O_2-sorption equilibria, structural identity and stability, thermal properties, as well as O_2-sorption kinetics and also studies of overall process performance. Although the sorption rate in this process is high, relative slowness of the desorption step may represent, at the time being, a major drawback of this type of sorbents. This issue may cause challenges with regard to achieving a high O_2-product purity in the industrial application of air separation needed for many purposes, and also to ensuring a sufficiently high efficiency of sorbent regeneration.[9] A TGA study of sorption and desorption kinetics in air-helium, *He*, systems showed that the rate of sorption may exceed that of desorption by about one order of magnitude.[6]

One important application of a perovskite-based production of an O_2-enriched CO_2 stream could be envisioned if CO_2 is used to replace O_2 from the sorbent column. The whole process could be described as follows: during the O_2-sorption process, air is used as the feed gas to saturate the sorbent with O_2, while CO_2 is swept through the column to desorb O_2 from the sorbent to obtain an O_2-enriched CO_2 gas as product.

This is a promising air-separation technique due to its great potential in the application of oxyfuel processes for fossil fuel combustion in power plants, cf.[10] From the viewpoint of pollution to the human environment, flue gas, which is produced when fuel is burnt in an O_2-CO_2 mixture instead of air, would mainly contain CO_2 but only small amounts of acid gases such as SO_x and NO_x, which would represent an easily met environmental issue rather than a major harm. That part of flue gas, which is almost entirely comprised of CO_2, could be used for coal transport or O_2 dilution, and would not attract unfavorable attention as greenhouse gas that causes global warming. Moreover, from the points of view of thermal efficiency and capital cost, an O_2-CO_2-blown combustion system accounts for a number of advantages: (1) no need would exist to separate CO_2 from flue gas; (2) the boiler efficiency would be improved; (3) power consumption in flue-gas treatment would be reduced because of only a small amount of flue gas involved; and (4) denitrification equipment could be spared.

The objective of this article is to understand several fundamental issues involved in the process for production of an O_2-enriched CO_2 stream by perovskite-type sorbents, and to illustrate feasibility of the underlying air-separation process.

Experimental Studies

Sorbent syntheses and characterization

The liquid citrate method followed by high-temperature sintering of reaction products was used to prepare sorbent material, $La_{0.1}Sr_{0.9}Co_{0.5}Fe_{0.5}O_{3-\delta}$, coded as LSCF, for this investigation. In general, this method is advantageous in preparing solid solution of multi-metal oxide with better control in stoichiometric composition, compared with the carbonate method. In the synthesis, metal-nitrate precursors were dissolved in deionized water according to final perovskite stoichiometry. Citric acid was added to that solution at 100% excess of the amount required for the reactions. During polymerization and condensation the system was heated and stirred at 100–105°C and 105–110°C, respectively. Water was gradually evaporated during condensation to facilitate gelation. At the end of the condensation step, viscous gel-like products were obtained. Self-ignition was performed at 400°C to burn off the organic components from synthesis products after they had been dried at 110°C for 24 h. Finally, as-prepared powders were sintered at 900°C for 20 h with a temperature-ramping rate of 60°C/h. As-prepared samples were ground into fine powders for fixed-bed experiments and characterization by TGA (SDT 2960 DSC/TGA system), and XRD (Siemens D-50 system with $CuK_{\alpha 1}$ radiation). Particle shapes and sizes of the samples were observed by SEM (Hitachi S-4,000). Average sizes of aggregated primary crystals of the materials were found to be about 10 μm.

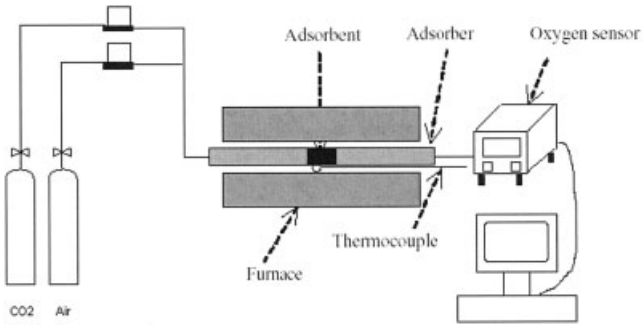

Figure 1. Fixed-bed setup used for sorption/desorption experiments.

Fixed-bed experiments

Air-separation experiments by sorption of O_2 on LSCF were conducted in a fixed bed. The experimental fixed-bed setup included a gas delivery system, an adsorber column, an O_2 analyzer (Ceramatec, Model 1100) and a computerized data-acquisition system, as shown in Figure 1.

Oxygen sorption and desorption breakthrough curves were recorded to study fixed-bed characteristics of the air-separation sorption process. The adsorber was a dense alumina tube of 6 mm i.d. and 9 mm o.d., loaded with 3.60 g of the LSCF powder described earlier. Dry air at 1 atm was used as the feed gas in the sorption step. During regeneration, helium or CO_2 was used as purge gases for column regeneration to compare their respective efficiencies towards replacement of O_2 from the LSCF column. The flow rates of sorption and desorption streams were kept at 5.00 ml/min for experiments at all temperatures. In the sorption step, the O_2 concentration of the effluent was determined by an O_2 sensor, as function of time after the feed gas was switched from the regeneration purge gas, He or CO_2, to air as sorption feed gas. Prior to sorption, the sorbent was exposed to regeneration at the same temperature over a time, ca. 48 h, sufficient to complete it. Desorption was conducted by sweeping the regeneration gas chosen at the same temperature. By recording the effluent O_2 concentration, fixed-bed air-separation breakthrough curves were obtained under various conditions over a range of temperature (500–800°C).

TGA experiments and XRD analysis

Phase-structure changes and reaction kinetics during sorption of O_2 from air and desorption in a CO_2 stream were studied by XRD (Siemens D-50 Cukα radiation) and TGA (TA Instru-

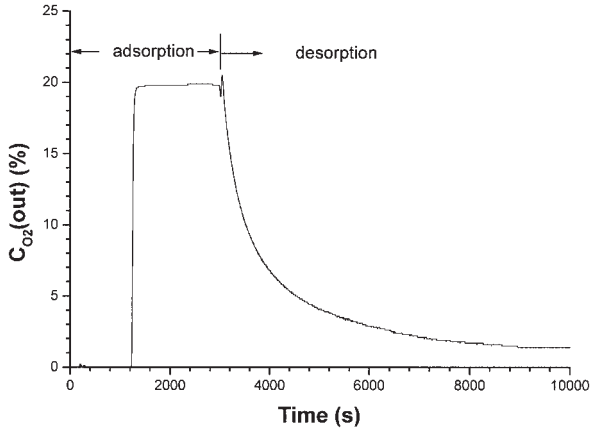

Figure 2. Oxygen sorption and desorption breakthrough curves for LSCF with He as desorption gas at 800°C.

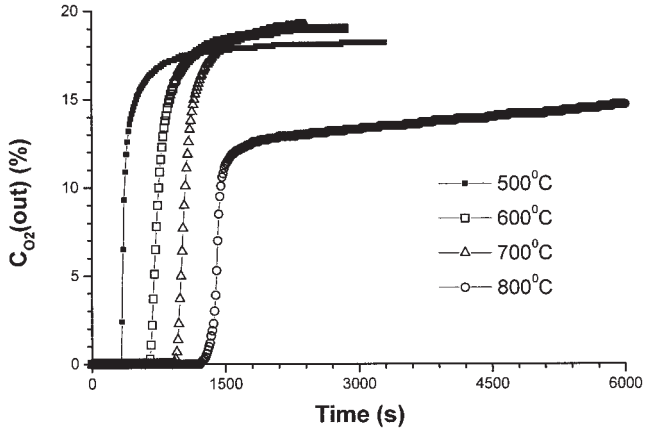

Figure 3. Oxygen sorption breakthrough curves for LSCF with CO_2 as desorption gas at (500–800)°C.

ment SDT/960) experiments, respectively. The experiments were started in the desorption mode, in which a fresh LSCF sample pre-equilibrated in air at a certain temperature, was exposed to CO_2 until reaching the new equilibrium state. Then the CO_2-purge stream was switched back to air to accomplish the subsequent O_2-sorption process. The weight change of the sample was recorded continuously throughout regeneration and sorption steps. To study the temperature effect on the reactions, TGA experiments were conducted in the temperature range of 500–800°C at a constant gas-flow rate of 100 mL/min.

The sorbent structure was examined by powder XRD after desorption and one cycle of reversed sorption/desorption steps. The examination began with desorption, during which a fresh LSCF powder sample was placed in the TGA instrument at 800°C in CO_2 stream at 100 ml/min for 17 days until its weight became stable (note that the baseline change in 17 days was less than 3% of the total weight change). Then the sample was quenched quickly to the ambient temperature by air cooling at a rate of about 200°C/min. Similarly, the reverted sorbent was obtained by placing the fresh LSCF in the TGA instrument in a CO_2 stream at flow rate of 100 mL/min and temperature of 800°C for several days, and then in an air stream at flow rate of 100 ml/min and temperature of 800°C for 10 days, until its weight became constant.

Results and Discussion

Fixed-bed sorption and regeneration characteristics

Both regeneration gases, He and CO_2, were used to examine their effects on the air-separation process utilizing LSCF sorbent. Sorption/desorption breakthrough curves were measured in fixed-bed experiments to compare their main sorption characteristics, for example, sorption capacity and desorption rate, over the temperature range of 500–800°C. Figure 2 presents a typical example for sorption/desorption breakthrough curves of O_2 at 800°C with He as regeneration gas.

A fast uptake process is witnessed by the steepness of the breakthrough curve for sorption, while the corresponding desorption curve exhibits a long tailing. This strongly asymmetric sorption/desorption behavior results from a highly favorable oxygen sorption isotherm of this material in connection with a low desorption rate.[1,3,4] Even lower desorption rates were observed at temperatures lower than 800°C.

Sorption breakthrough curves for O_2 in 500–800°C, after having used CO_2 as regeneration gas, are presented in Figure 3. Related desorption breakthrough curves with CO_2 for regeneration are shown in Figure 4.

A two-step sorption process in air separation was observed in 500–800°C, viz., a first fast stage was followed by a second stage with significantly slower O_2 uptake. This result is different from that with He as purge gas that exhibits a fast rate over the entire sorption process. However, apparently different from desorption by He purge, a much faster process could be observed from desorption curves at 700 and 800°C. The improved desorption is not observed at 500 and 600°C, which is due to the slow kinetics of the reaction between CO_2 and the sorbent, as will be demonstrated later by the results of TGA kinetic study at different temperatures.

Figure 5 offers a comparison of breakthrough curves for desorption between He and CO_2 at 800°C. For CO_2, an O_2 concentration up to 75% was found over desorption time of 600–800 s, and it remained above 20% level before desorption time extended towards 2,500 s. However, for desorption with

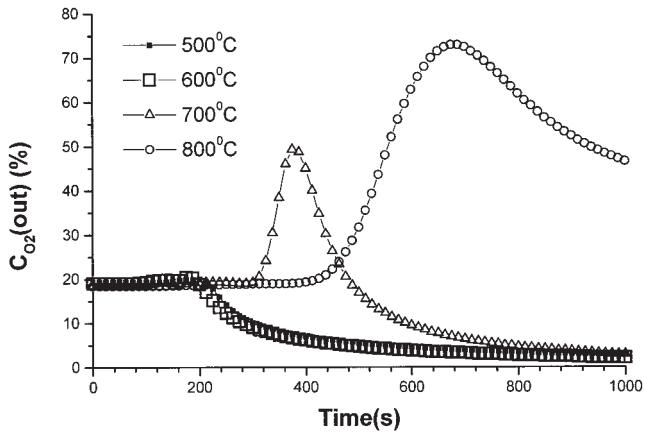

Figure 4. Desorption breakthrough curves for LSCF with CO_2 as desorption gas at (500–800)°C.

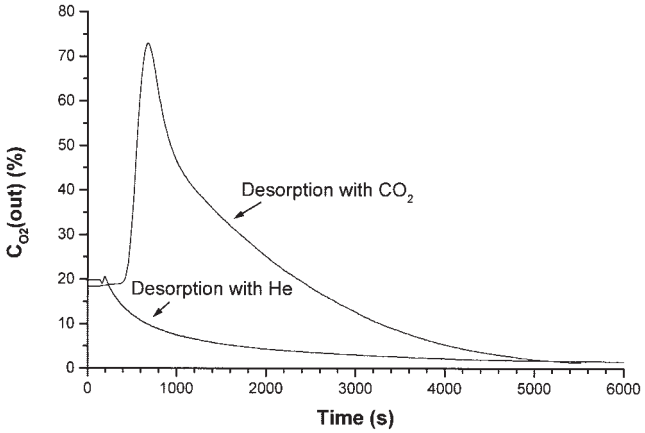

Figure 5. Desorption processes with CO_2 and He at 800°C.

He purge, the O_2 concentration dropped quickly to a level below 5% after about 250 s. This indicates a much faster oxygen desorption process with CO_2 purge than with He purge.

For the desorption step, an average desorption rate between times t_1 and t_2, r_d, is used to illustrate the relative desorption rate. It was obtained from a desorption breakthrough curve by the following mass balance equation

$$r_d = \frac{1}{RT(t_2 - t_1)m_s} \int_{t_1}^{t_2} (F_{o,t}X_{o,t}P_o)dt \tag{1}$$

where m_s is the amount of sorbent packed; $F_{o,t}$, P_o, and $X_{o,t}$ are total volumetric flow rate, total pressure, and molar percentage of O_2 in the effluent. T is the effluent temperature (the room-temperature in this study). For the sorption step, oxygen sorption capacity up to the time t, Q_a, was calculated from a sorption breakthrough curve by

$$Q_a = \frac{1}{RTm_s} \int_0^t (F_iX_iP_i - F_{o,t}X_{o,t}P_o)dt \tag{3}$$

where the subscript i indicates the properties in the feed. The total effluent flow rate was measured by a mass flow meter or estimated (with He as the desorption gas) from the total feed flow rate, F_i, by

$$F_{o,t} = \frac{F_i(1 - X_i)}{1 - X_{o,t}} \tag{3}$$

Table 1 compares average desorption-rate data for O_2 over various time ranges on LSCF with He and CO_2 as desorption gases. As seen from Table 1, LSCF exhibits much higher integral desorption rate using CO_2 as sweeping gas, compared to the case with He. Especially at 800°C, the desorption rate with CO_2 at $t < 1{,}000$ s is ca. 10 times that with He, and it keeps increasing within $1{,}000 < t < 2{,}000$ s to ca. 500 times higher than that with He. During desorption by He, the rate drops quickly to almost 0.5×10^{-6} mmol g^{-1} s^{-1} after 1,000 s at all temperatures. It would take ca. 48 h to complete sorbent regeneration at such rate, if possible at all.

Table 1. Comparison of Desorption Rates of LSCF Using He and CO_2 Regeneration at Different Temperatures and in Different Time Ranges

Temperature (°C)	Time Range (s)	Desorption Rate with CO_2 r_d (mmol/g.s) × 10^6	Desorption Rate with He r_d (mmol/g.s) × 10^6
500	0–1000	37	15
	1000–2000	21	<0.1
600	0–1000	37	18
	1000–2000	20	<0.5
700	0–1000	56	20
	1000–2000	13	<0.5
800	0–1000	162	20
	1000–2000	250	<0.5

Table 2 offers a comparison of O_2-sorption capacities, Q_a, of LSCF between CO_2, and He as sweeping gases. Due to the slow rate for the second stage of the sorption process with CO_2 as sweeping gas (it may take 12 h to complete a breakthrough curve), cf., Figure 3, the sorption capacity measured over the time interval, $0 - t$, represents only an incomplete sorption capacity. It is compared with the total sorption capacity as found by sweeping with He. As seen from Table 2, though the sorption capacity calculated with CO_2 as desorption sweeping gas amounts only to a part of the total sorption capacity, it is still larger than the total sorption capacity with He as sweeping gas. Especially at 800°C, the sorption capacity is larger by about one order of magnitude.

The oxygen sorption capacity with helium as the desorption gas is related to the difference of equilibrium oxygen nonstoichiometry for LSCF between air and He.[1] This difference may increase or decrease with temperature. The data for He in Table 2 shows that the sorption capacity decreases and then increases with increasing temperature. Such temperature dependency for the oxygen sorption capacity is fairly common for this group of materials.[1] At 500 and 600°C, the reaction rate between CO_2 and LSCF is slow and CO_2 acts similar to He in regenerating the LSCF sorbent. This gives similar oxygen sorption capacities for the cases of CO_2 and He in the low temperature range. At 700 and 800°C the reaction rate between CO_2 and LSCF is much enhanced. As a result LSCF is regenerated effectively through a chemical reaction. Thus, in the high-temperature range, this gives much larger oxygen sorption capacity with CO_2 as desorption gas than with He.

To assess the reversibility of sorption/desorption processes of the system investigated, six consecutive sorption cycles were performed after long-time preregeneration under the

Table 2. O_2 Sorption Capacities of LSCF with CO_2 and He as Sweeping Gases

Temperature °C	Sorption Capacity (Not Completely) with CO_2 Q_a (mmol/g)	Total Sorption Capacity with He Q_a (mmol/g)
500	0.347	0.345
600	0.318	0.316
700	0.637	0.218
800	2.388	0.248

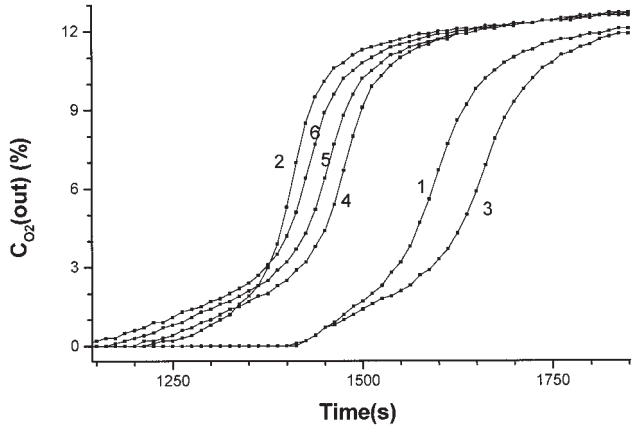

Figure 6. Six cycles of sorption breakthrough curves with CO_2 as desorption gas at 800°C.

fixed-bed conditions. The results of these experiments are shown in Figure 6. The breakthrough curves exhibit breakthrough fronts that are similar to each other, though there is a difference in sorption rates for several of them. This difference could be understood by considering results compiled in Table 3 that allows for a comparison of apparent sorption capacities reached after 1,600 s in each of those cycles, and accounting for the particular desorption time.

The differences in apparent sorption capacities are due to differences in the lengths of the preceding desorption steps prior to each sorption cycle or differences in the amount of the oxygen desorbed during the desorption step, as confirmed by a mass balance on oxygen for each cycle. Long desorption time results in larger O_2-sorption capacities reached after 1,600 s. This finding implies that the cycle "air sorption-CO_2 desorption" on LSCF shows good reversibility. If assuming that each cycle would have been conducted with complete regeneration by CO_2, they should exhibit identical sorption breakthrough curves with identical sorption-capacity values. Complete regeneration would mean that further extension of desorption time does not allow for additional desorption of O_2.

Phase-structure change of LSCF after sorption and desorption with CO_2

Figure 7 shows the XRD pattern of LSCF after reaching desorption equilibrium at temperature of 800°C. Compared to the XRD pattern of a fresh LSCF sample, main characteristic peaks of the perovskite structure still exist. Besides, it also shows the main characteristic peaks of the $SrCO_3$ structure. The remaining peaks match those of La_2O_3, $Fe_{21.34}O_{32}$ (representing practically Fe_2O_3), and CoO, respectively. Table 4 compiles data to prove the degree of matching of the XRD peaks of solid products after desorption, and their main characteristic peaks at 800°C.

According to this XRD analysis, LSCF undergoes a carbonation reaction that leads to the formation of $SrCO_3$, La_2O_3, $Fe_{21.34}O_{32}$, and CoO as solid products and O_2 in accordance with the following equation

$$La_{0.1}Sr_{0.9}Co_{0.5}Fe_{0.5}O_{2.6} + 0.9\ CO_2 \Leftrightarrow 0.9\ SrCO_3 + 0.05\ La_2O_3 + 0.5\ CoO + 0.25\ Fe_2O_3 + 0.15\ O_2 \quad (B)$$

Due to the material balance expressed by this reaction, O_2 is produced as an LSCF-carbonation product. This explains the occurrence of O_2 in the effluent gas of the fixed-bed experiments described, cf., Figure 7.

The sorbent-weight increase found in conjuncture with the desorption (carbonation) process gives a further proof of evidence for the formation of $SrCO_3$ and metal oxides. In addition, the weight-increase ratio calculated theoretically from Eq. B, which was derived from XRD analysis, is consistent with the experimental weight-increase ratio for the related long-time desorption process, that is, over ca. 10 days. The theoretical weight increase due to reaction B amounts to 18.2 wt.%, while the weight increase at 700°C from TGA experiments is 14.3 wt.%. The difference between those weight-increase values should be ascribed to incompleteness of experimental desorption under TGA conditions, although that process lasted over 10 days. Presence of partly undestroyed perovskite structure shown by the XRD pattern of the solid desorption products after carbonation at 800°C supports this explanation, cf., Figure 7 and Table 4.

Figure 8 shows a comparison of XRD patterns of a fresh LSCF sample and a reverted product after processes of complete desorption (carbonation) and subsequent complete sorption (oxygenation) 800°C. As seen therefrom, the reverted product exhibits a perfect XRD pattern with all the main peaks characteristic of a perovskite structure. Thus, the solid desorption products revert into a perovskite structure after undergoing a complete O_2-sorption process.

Kinetics of the carbonation reaction

Figure 9 shows CO_2-uptake curves on LSCF at various temperatures. These curves exhibit a fast initial reaction rate (within the first 1,000 min), and a gradual transition to a much slower reaction rate before reaching equilibrium.

This feature could be relevant for a practical utilization of LSCF in an O_2-separation application. The first fast reaction stage could be used for the O_2-desorption process. Since this process also delivers O_2 when the perovskite-structured sorbent reacts with CO_2, the faster the rate, the higher the O_2 concentration in the mixture of CO_2 yielded by the desorption process. The reaction rate is the fastest at the beginning, which results in the maximum oxygen concentration in the desorption effluent, as shown in the desorption breakthrough curves at 700 and 800°C in Figure 4. After that, the reaction rate decreases with time, leading to a decrease in the effluent oxygen concentration as well.

In addition, Figure 10 also indicates an enhancement of the first-stage reaction rate, i.e., over 500 min, by increasing temperature. This is consistent with a conclusion from desorption-

Table 3. Comparison of Sorption Capacities after 1,600 s of Six Sorption Cycles with their Preliminary Desorption Time

Cycle	Sorption Capacity (Q_a before 1600 s, mmol/g)	Preliminary Desorption Time (h)
1	0.291	20.3
2	0.273	16.6
3	0.293	120.0
4	0.279	18.0
5	0.276	17.0
6	0.273	16.8

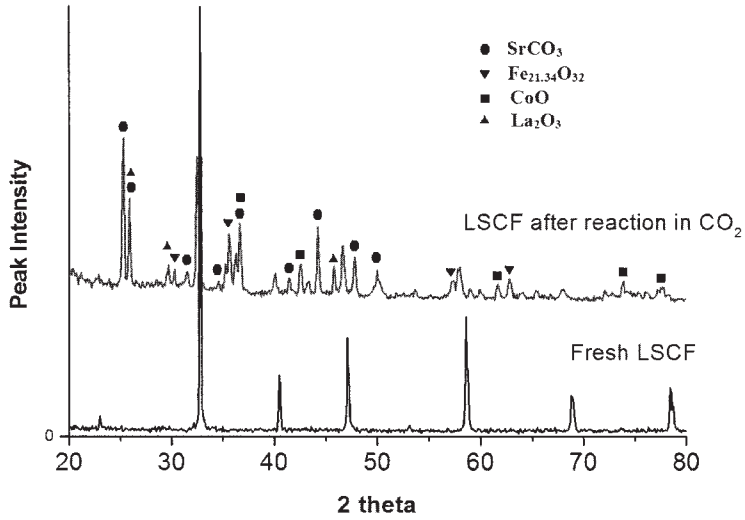

Figure 7. XRD patterns of solid desorption products with CO_2 as desorption gas at 800°C.

breakthrough curves shown in Figure 5, which refers to the observation of increase in O_2 concentration in the effluent with increase in temperature. For example, at temperature of 800°C the process yields ca. 75% of O_2 in the effluent, whereas at 600°C it yields ca. 24% at the most. This means that temperature affects significantly the carbonation-reaction kinetics. At $T < 600$°C, no effective O_2-desorption process takes place. However, the reaction rate becomes rather fast at $T > 700$°C, which results in much better O_2-separation effect, as witnessed by high O_2-concentration in the effluent gas in accordance with desorption-breakthrough curves measured at 700 and 800°C.

Figure 10 shows CO_2 desorption (or O_2 sorption) break-

Table 4. Comparison of XRD Patterns of Perovskite Type Sorbent after Regeneration with CO_2 at 800°C with Standard XRD Peaks

Material	XRD Peaks *d* (A)	Peak Intensity (%)	Standard Characteristic Peaks for Pure Material *d* (A)	Peak Intensity for Pure Material (%)	(*h k l*)
Perovskite structure of LSCF (Cubic)	2.746	100	2.713	100	(1 1 0)
	2.248	22	2.214	14	(1 1 1)
	1.945	41	1.916	27	(2 0 0)
	1.591	27	1.568	25	(2 1 1)
	1.371	12	1.359	11	(2 2 0)
$SrCO_3$ ISCD#: 027293 (Orthorhombic)	3.529	100	3.527	100	(1 1 1)
	3.438	64	3.438	51	(1 0 2)
	2.830	21	2.832	10	(2 0 1)
	2.589	15	2.591	7	(2 1 0)
	2.545	25	2.546	14	(0 2 0)
	2.479	32	2.475	23	(2 1 1)
	2.451	50	2.448	28	(0 1 3)
	2.044	47	2.046	36	(2 0 3)
	2.178	17	2.176	9	(0 2 2)
	1.900	29	1.899	23	(2 1 3)
	1.823	22	1.822	19	(3 1 1)
$Fe_{21.34}O_{32}$ ICSD#: 079196 (Cubic)	2.947	52	2.951	36	(2 2 0)
$Fe_{21.34}O_{32}$ ICSD#: 079196 (Cubic)	2.947	52	2.951	36	(2 2 0)
	2.513	100	2.516	100	(3 1 1)
	2.087	35	2.087	18	(4 0 0)
	1.604	40	1.606	25	(5 1 1)
	1.477	40	1.475	36	(4 4 0)
CoO ICSD#: 029226 (Cubic)	2.451	196	2.450	68	(1 1 1)
CoO ICSD#: 029226 (Cubic)	2.451	196	2.450	68	(1 1 1)
	2.121	100	2.122	100	(2 0 0)
	1.503	54	1.500	45	(2 2 0)
	1.282	61	1.280	16	(3 1 1)
	1.229	47	1.225	11	(2 2 2)
La_2O_3 ICSD#: 100204 (Hexagonal)	3.438	257	3.411	30	(1 0 0)
La_2O_3 ICSD#: 100204 (Hexagonal)	3.438	257	3.411	30	(1 0 0)
	3.003	100	2.981	100	(0 1 1)
	1.981	98	1.969	30	(1 1 0)

(2000 JCPDS-International Center for Diffraction Data. v.2.1).

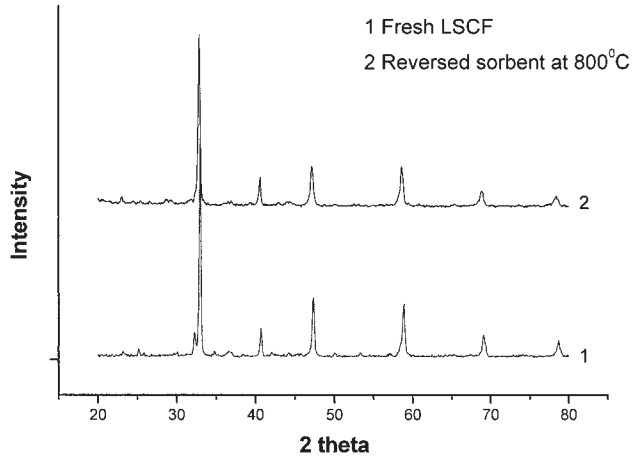

Figure 8. XRD patterns of fresh LSCF sorbent and its reverted products after carbonation at 800°C.

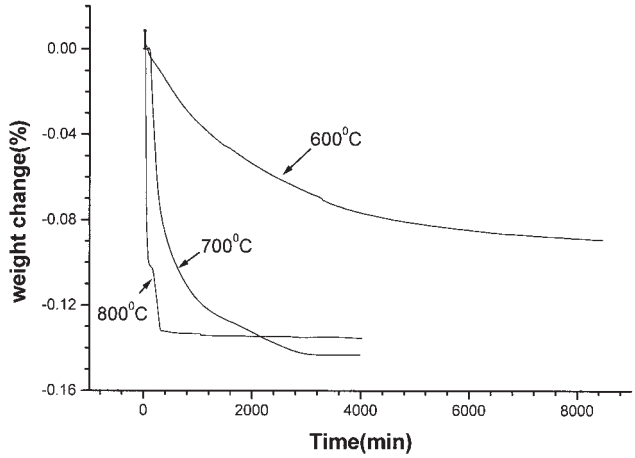

Figure 10. CO_2 desorption (O_2 sorption) curves on the carbonation product in air stream at various temperatures.

through curves for the fixed-bed packed with carbonated LSCF with air as the feed at various temperatures. This process comprises just the reverse of the carbonation reaction referred earlier: (1) the solid carbonation products absorb O_2 and retransform into the perovskite-type material LSCF, which releases CO_2 in the meanwhile; (2) the reverse reaction proceeds at a higher rate than the carbonation reaction over the entire reaction process; (3) the reaction rate depends strongly on temperature, that is, it is much faster at 700 and 800°C compared to that at 600°C, at which even 17,000 min seem to be an insufficient time to complete the reversion. Since the reverse reaction should be applied to sorbent regeneration, its rate represents a significant feature of an overall process. Thus, an optimum temperature for regeneration of LSCF should be higher than 700°C. It should be noted that during a high-temperature cyclic process of production of O_2-CO_2 mixtures (with O_2 enrichment due to air separation), the decomposition of perovskite-type sorbent would effectively be suppressed since the O_2-sorption reaction, which heals the perovskite structure, proceeds at significantly higher rate than the desorption (carbonation) reaction, which decomposes (reversibly) the perovskite structure.

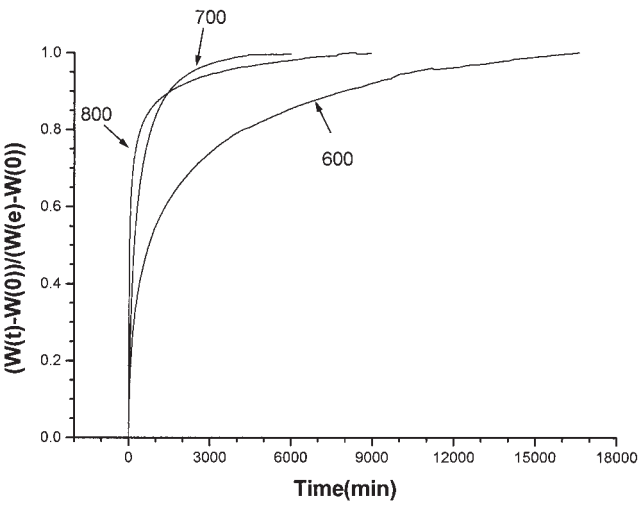

Figure 9. CO_2 uptake curves on the LSCF sorbent at various temperatures.

Conclusions

Properties of sorption/desorption processes for the perovskite-type ceramic sorbent $La_{0.1}Sr_{0.9}Co_{0.5}Fe_{0.5}O_{3-\delta}$ was studied in its application for the production of an oxygen-enriched carbon dioxide. A high desorption efficiency and good reversibility were achieved by using CO_2 as desorption sweeping gas. This desorption process exhibits an average rate exceeding that with inert gas such as helium as desorption gases by a factor of about 500 at a temperature of 800°C. The sorption/desorption processes are completely reversible. The perovskite LSCF undergoes a structure change during the desorption process. This structure change is found to be entirely reversible during the sorption process. The reversible process can be expressed by the following formula

$$La_{0.1}Sr_{0.9}Co_{0.5}Fe_{0.5}O_{2.6} + 0.9\ CO_2 \Leftrightarrow 0.9\ SrCO_3 + 0.05\ La_2O_3 + 0.5\ CoO + 0.25\ Fe_2O_3 + 0.15\ O_2$$

The kinetics of both the direct (carbonation) and reverse (oxygenation) reactions exhibit a fast reaction-rate step followed by a gradual transition to a step with slower rate, which needs a comparatively long time to reach equilibrium. The reaction rate has a positive temperature increment. A remarkable efficiency is observed at temperature of 800°C.

Acknowledgments

The project was partly supported by National Science Foundation (CTS-0132694), Department of Energy (DE-FG26-00NT4081) and the BOC Group.

Literature Cited

1. Yang ZH, Lin YS, Zeng Y. High temperature sorption process for air separation and oxygen removal. *Ind & Eng Chem Res.* 2002;41:2775.
2. Zeng Y, Wolf RJ, Fitch FR, Bülow M, Tamhankar S, Acharya DR. Supported Perovskite-type Oxides and Methods of Preparation Theory. US Patent Application 2002/0179887, publ. Dec 5; 2002.

3. Mizusaki J, Mima Y, Yamauchi S, Fueki K, Tagawa H. Nonstoichiometry of the perovskite-type oxides $La_{1-x}SrxCoO_{3-\delta}$. *J of Solid State Chem.* 1989;80(1):102–111.
4. Mizusaki J, Yamauchi S, Fueki K, Ishikamw A. Nonstoichiometry of Perovskite-type Oxides $La_{1-x}Sr_xCoO_{3-\delta}$. *Solid State Ionics.* 1984;12: 119–124.
5. Bouwmeester HJM, Burggraaf AJ, Gellings PJ, Bouwmeester HJM (Eds.), *Solid State Electrochemistry.* Boca Raton: CRC Press; 1997.
6. Yang ZH. *High Temperature Sorption Process for Air Separation and Oxygen Removal.* Cincinnati: University of Cincinnati; 2002. Ph.D. Dissertation.
7. Dyer PN, Richards RE, Russek SL, Taylor DM. Ion transport membrane technology for oxygen separation and syngas production. *Solid States Ionics.* 2000;134:21–33.
8. Lin YS, McLean DL, Zeng Y. High Temperature Sorption Process for Air Adsorption Process. US Patent 6,059,858, 2000.
9. Yang RT. *Gas Separation by Adsorption Processes.* Boston: Butterworths; 1987.
10. Horlock JH. *Advanced Gas Turbine Cycles.* Oxford: Pergamon; 2003.

Manuscript received Feb. 20, 2005, and revision received Jun. 18, 2005.